substance: boron compounds with lanthanides
property: properties of LaB_4 type compounds

(See also document on **structural properties of tetraborides with B_6 octahedra)**

Structure type tP20-ThB_4

Space group: P4/mbm

lattice parameters
(in Å)

a	7.3246	*T* = 300 K	X-ray diffraction	71D
c	4.1809			
a	7.324	*T* = 300 K	X-ray diffraction	74K
c	4.181			
a	7.3248(8)	*T* = 300 K	sample6, X-ray diffraction	90B
	7.32804		sample7, X-ray diffraction	
c	3.822(1)		sample6	
	4.1829(5)		sample7	

Density of states calculation in Fig. 1 [86B1].

Entropy [86B2].

melting point

T_m	1800 °C	melting with decomposition	96G

CeB_4

melting point

T_m	2380 °C	melting with decomposition	96G

Entropy in [86B2].

standard enthalpy of formation

ΔH_f^0	–53.5(15) kJ/g atom	synthesis calorimetry from the elements	95M, 93M

PrB_4

melting point

T_m	~2350 °C	melting with decomposition	96G

Entropy in [86B2].

standard enthalpy of formation

ΔH_f^0	–53.1(16) kJ/g atom	synthesis calorimetry from the elements	95M, 93M

NdB_4

melting point

T_m	~2350 °C	melting with decomposition	96G

Entropy in [86B2].

standard enthalpy of formation

ΔH_f^0	–53.3(15) kJ/g atom		synthesis calorimetry from the elements	95M

PmB_4

melting point

T_m	~2350 °C		melting with decomposition	96G

SmB_4

melting point

T_m	~2400 °C		melting with decomposition	96G

Entropy in [86B2].

microhardness
(in kg mm^{-2})

H_K(prism)	2130...2610	T = 300 K	load 50 g	96G
H_K(pinacoid)	1860...2600		(range of anisotropy)	

EuB_4

microhardness
(in kg mm^{-2})

H_K(prism)	1900...2020	T = 300 K	load 50 g	96G
H_K(pinacoid)	1430		α = 45° (α = angle between the direction of the long diagonal of the Knoop pyramid and the edge of the investigated face)	

GdB_4

Entropy in [86B2].

microhardness
(in kg mm^{-2})

H_K(prism)	2120...2490	T = 300 K	load 50 g	96G
H_K(pinacoid)	1610...2050		(range of anisotropy)	

Magnetic susceptibility in Fig. 2.

TbB_4

Structure: tetragonal

Space group: P4/mbm

Preparation by Czochralski and aluminium flux methods; anisotropy and magnetic properties in [81G].

Neutron diffraction study in [76S].

lattice parameters
(in Å)

a	7.120(3)	T = 300 K	neutron diffraction	81W
c	4.042(2)			
c/a	0.5677			
V	204.9(2) $Å^3$			

Temperature dependence of the lattice parameters indicating a phase transition at 80K in Fig. 3 [86W].

phase transition

T_{tr}	80K	tetragonal to orthorhombic structure	86W

Temperature dependence of resistivity, thermoelectric power, Hall coefficient in Fig. 4 [75P].

magnetic parameters

T_N	45 K	81G
	43 K	86W
Θ_p	−30 K	81G

Antiferromagnetic structure in Fig. 5 [86W, 81W].

Temperature dependence of the reciprocal magnetic susceptibilities of a single crystal $\chi_{\parallel}^{-1}$ and $\chi_{\perp}^{-1}$ (H = 3000 Oe) in Fig. 6 [81G].

Variation of the magnetization as a function of field applied perpendicular to the *c* axis of a single crystal at 4.2 K in Fig. 7 [81G].

microhardness
(in kg mm^{-2})

H_K(pinacoid)	1850...25300	T = 300 K	load 50 g	96G
H_K(prism)	1610...2050		(range of anisotropy)	

melting point

T_m	~2600 °C	96G

DyB_4

melting point

T_m	~2500 °C	96G

microhardness
(in kg mm^{-2})

H_K(prism)	1690...2120	T = 300 K	load 50 g	96G
H_K(pinacoid)	1950...2000		(range of anisotropy)	

HoB_4

Preparation by Czochralski and aluminium flux methods; anisotropy and magnetic properties in [81G].

magnetic parameters

T_N	9 K	81G
Θ_p	−10 K	
$\Theta_{p\parallel}$	−9.8 K	
$\Theta_{p\perp}$	−13.4 K	

Variation of the magnetization as a function of field applied normal to the *c* axis at different temperatures in [81G].

Magnetic susceptibility in Fig. 2.

Temperature dependence of the reciprocal magnetic susceptibilities $\chi_{\parallel}^{-1}$ and $\chi_{\perp}^{-1}$ in in Fig. 8 [81G].

Variation of the magnetization as a function of field applied parallel to the *c* axis at 2.25 K in Fig. 9 [81G].

Variation of the magnetization as a function of field applied normal to the c axis at different temperatures in Fig. 10 [81G].

microhardness
(in kg mm^{-2})

H_K(prism)	1990...2680	T = 300 K	load 50 g	96G
H_K(pinacoid)	1500...1990		(range of anisotropy)	

melting point

T_m	~2500 °C	96G

ErB_4

Structure: tetragonal

Space group: P4/mbm

Phase transition temperatures: crystallographic (tetragonal to orthorhombic) at 80K; magnetic at T_N = 43 K.

Preparation by Czochralski and aluminum flux methods [81G].

Neutron diffraction analysis in [81E].

Neutron diffraction study in [81W].

Structure investigation (boron-rich corner of the Er-Al-B system) in [94Y].

lattice parameters
(in Å)

a	7.071(1)	*T* = 300 K	neutron diffraction	81W
c	4.000(1)			
c/*a*	0.5657			
V	200.0(1) $Å^3$			
a	7.0791(14)	*T* = 4.2 K	X-ray diffraction	86W
b	7.0765(14)			
c	3.9931(3)			

magnetic parameters

T_N	13 K	81G
Θ_p	–5 K	
$\Theta_{p\|\|}$	13 K	
$\Theta_{p\perp}$	–18 K	

Antiferromagnetic structure with the magnetic moments oriented parallel to the *c* axis in Fig. 11 [81W, 86W, 81W].

Magnetic susceptibility in Fig. 2 [74P].

Magnetic phase diagram in Fig. 12 [81G].

Anisotropy and magnetic properties in [81G].

melting point

T_m	~2500 °C	96G

microhardness
(in kg mm^{-2})

H_K(prism)	2230...2730	T = 300 K	load 50 g	96G
H_K(dipyramid)	1920...2500		(range of anisotropy)	
H_K(pinacoid)	1700...1990		(range of anisotropy)	

TmB_4

Structure: tetragonal

Space group: P4/mbm

lattice parameters

a	7.0550(3) Å	T = 300 K	X-ray diffraction	94O2
c	3.9870(3) Å			

For lattice parameters see also [91K, 90M].

resistivity

ρ	$0.119 \cdot 10^{-3}$ Ω cm	T = 300 K		92O, 94O1

melting point

T_m	~2550 °C			96G

microhardness

H_V	17.1...18.7 GPa	T = 300 K		92O, 94O1
	16.8...18.3 GPa		load 100 g	94O2
	2130 kg mm^{-2}		dipyramid, load 50 g	96G

YbB_4

Structure: tetragonal

Space group: P4/mbm

Single crystal preparation by the aluminum-flux method [94O1].

lattice parameters

a	7.0612(5) Å	T = 300 K		94O1
c	3.9893(3) Å			
V	198.91(6) Å^3			

density
(in g cm^{-3})

d	7.15(5)	T = 300 K	pycnometric	94O1
	7.222(3)		X-ray	

resistivity

ρ	$0.26 \cdot 10^{-3}$ Ω cm	T = 300 K		94O1

melting point

T_m	~2550 °C		melting with decomposition	96G

LuB_4

Structure: tetragonal

Space group: P4/mbm

Prepartion of single crystals by the high-temperature aluminum solution method [96O].

lattice parameters

a	0.7035(1) nm	*T* = 300 K	X-ray diffraction	96O
c	0.3975(3) nm			
V	0.1967 nm^3			

References:

71D Deacon, J.A., Hiscocks, S.E.R.: J. Mater. Sci. 3 (1971) 309.

74K Kato, K., Kawada, I., Oshima, C., Kawai, S.: Acta Crystallogr. B 30 (1974) 2933.

74P Paderno, Yu.B., Severianina, E.N., Fedchenko, S.G.: Neorg. Mater. 10 (1974) 1900.

75P Paderno, Yu.B., Severianina, E.N., Dudnik, E.M., Lazorenko, V.I.: in: Refractory alloys of metals with special physica-chemical properties, Izdatel'stvo NAUKA ed., Moscow, 1975, p. 118 (in Russian).

76S Schäfer, W., Will, G., Buschow, K.H.J.: J. Chem. Phys. 64 (1976) 1994 (neutron diffraction study on ErB_4).

81E Elf, F., Schäfer, W., Will, G., Etourneau, J.: Solid State Commun. 40 (1981) 579 (neutron diffraction studies of TbB_4).

81G Gianduzzo, J.C., Georges, R., Chevalier, B., Etourneau, J., Hagenmuller, P., Will, G, Schäfer, W., Elf, F.: J. Less-Common Met. 82 (1981) 29. (Proc. 7th Int. Symp. Boron, Borides and Rel. Compounds, Uppsala, Sweden, 1981).

81W Will, G., Schäfer, W., Pfeiffer, F., Elf, F., Etourneau, J.: J. Less-Common Met. 82 (1981) 349 (Proc. 7th Int. Symp. Boron, Borides and Rel. Compounds, Uppsala, Sweden, 1981).

86B1 Bullett, D.W.: in: Boron-Rich Solids (AIP Conf. Proc. 140), Albuquerque, New Mexico 1985, D. Emin, T.L. Aselage, C.L. Beckel, I.A. Howard ed., American Institute of Physics: New York, 1986, p. 249.

86B2 Borovikova, M.S., Fesenko, V.V.: J. Less-Common Met. 117 (1986) 287. (Proc. 8th Int. Symp. Boron, Borides, Carbides, Nitrides and Rel. Compounds, Tbilisi, Oct. 8 - 12, 1984)

86W Will, G., Heiba, Z., Schäfer, W., Jansen, E.: in: Boron-Rich Solids (AIP Conf. Proc. 140), Albuquerque, New Mexico 1985, D. Emin, T.L. Aselage, C.L. Beckel, I.A. Howard ed., American Institute of Physics: New York, 1986, p. 130.

90B Bolmgren, H., Lundström, T.: J. Less-Common Met. 163 (1990) 79.

90M Massalski, T.B.: in: Binary alloy phase diagrams, He Materials Information Society ed., ASM International: Ohio, 1990 (2nd ed.).

91K Korsukova, M.M.: in: Boron-Rich Solids, Proc. 10th Int. Symp. Boron, Borides and Rel. Compounds, Albuquerque, NM 1990 (AIP Conf. Proc. 231), D. Emin, T.L. Aselage, A.C. Switendick, B. Morosin, C.L. Beckel ed., American Institute of Physics: New York, 1991, p. 232.

92O Okada, S., Kudou, K., Lundström, T.: in: Proc. Cryst. Conf. Osaka, Osaka, 1992, p. 103.

93M Meschel, S.V., Kleppa, O.J.: Metall. Trans. A 24 (1993) 947.

94O1 Okada, S., Kudou, K., Yu, Y., Lundström, T.: Proc. 11th Int. Symp. Boron, Borides and Rel. Compounds, Tsukuba, Japan, August 22 - 26, 1993, Jpn. J. Appl. Phys. Series 10 (1994), p. 136.

94O2 Okada, S., Kudou, K., Yu, Y., Lundström, T.: Jpn. J. Appl. Phys. 33 (1994) 2663.

94Y Yu, Y., Lundström, T.: J. Alloys Compounds 210 (1994) 191.

95M Meschel, S.V., Kleppa, O.J.: J. Alloys Compounds 221 (1995) 37.

96G Gurin, V.N., Derkachenko, L.I., Korsukova, M.M., Nikanorov, S.P., Jung, W., Müller, R.: Sov. Phys. Solid State 38 (1996) 1508.

96O Okada, S., Yu, Y., Lundström, T., Kudou, K., Tanaka, T.: Jpn. J. Appl. Phys. 35 (1996) 4718.

Fig. 1.

LaB_4. Electron density of states calculation [86B1]. The lower curve indicates the projection on metal atoms; the arrow indicates the Fermi level.

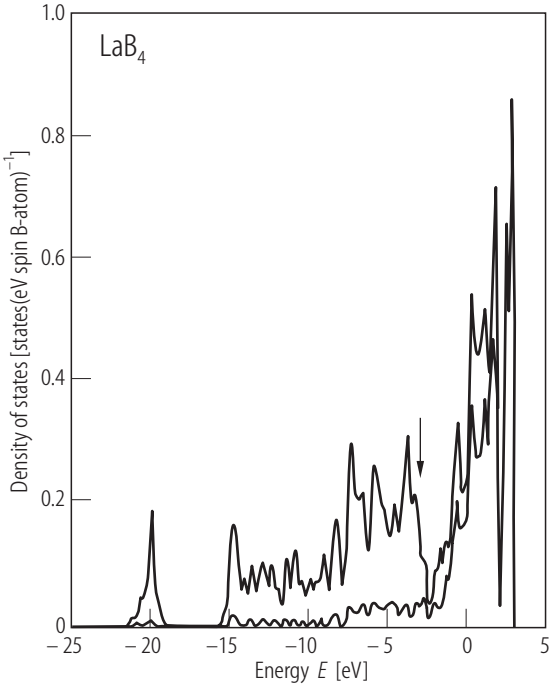

Fig. 2.

Metal tetraborides (GdB_4, HoB_4, ErB_4). Reciprocal magnetic susceptibility vs. *T* [74P].

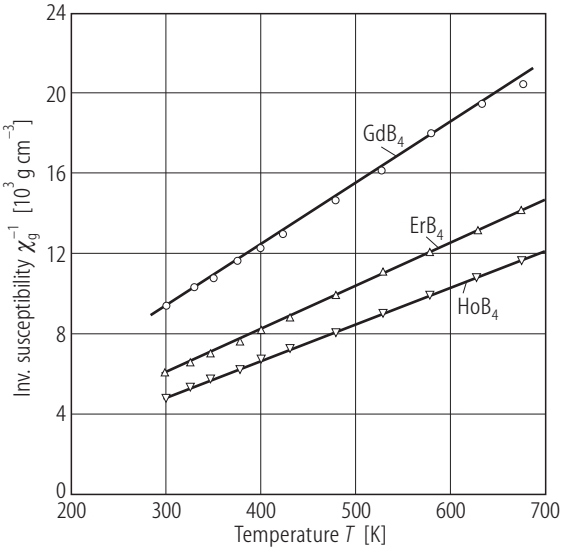

Fig. 3.

TbB_4. Temperature dependence of the lattice parameters indicating a phase transition at 80K [86W].

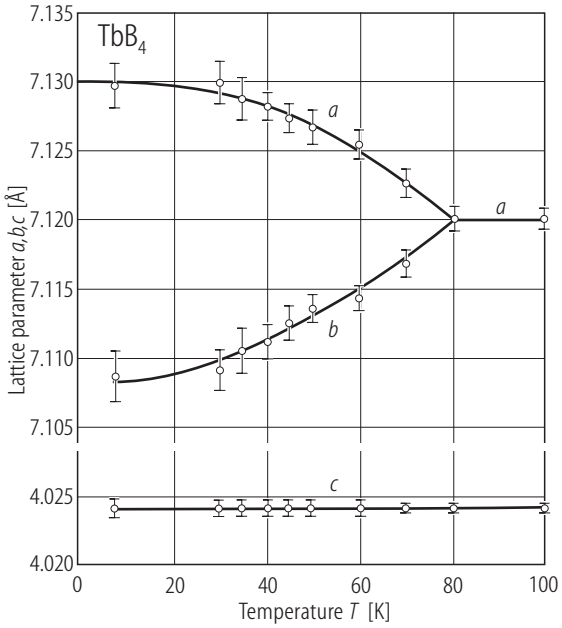

Fig. 4.

TbB_4. Temperature dependence of resistivity, thermoelectric power and Hall coefficient [75P].

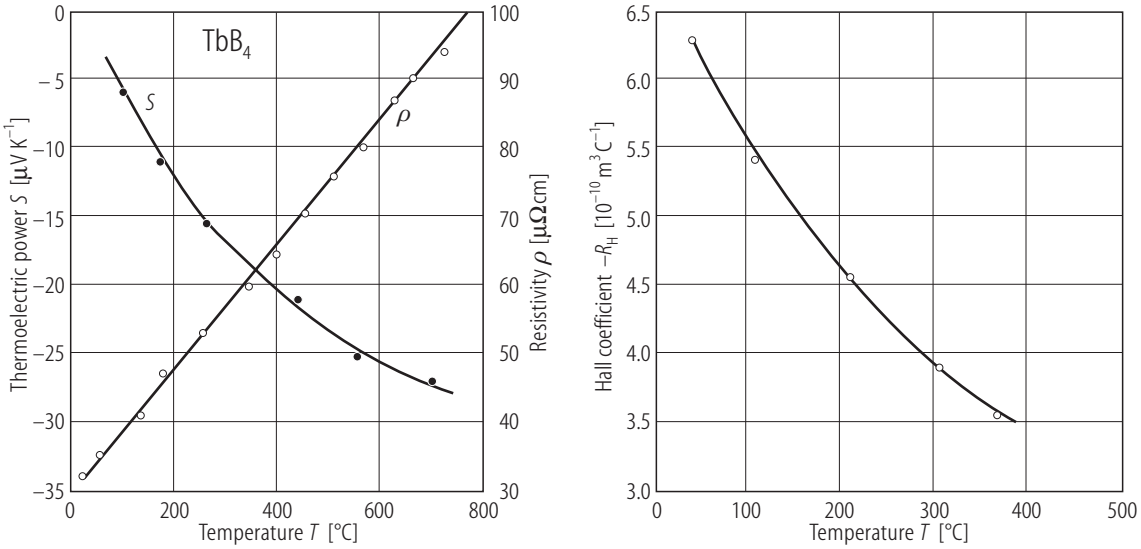

Fig. 5.

TbB_4. Antiferromagnetic structure with the magnetic moments oriented perpendicular to the *c* axis [81W].

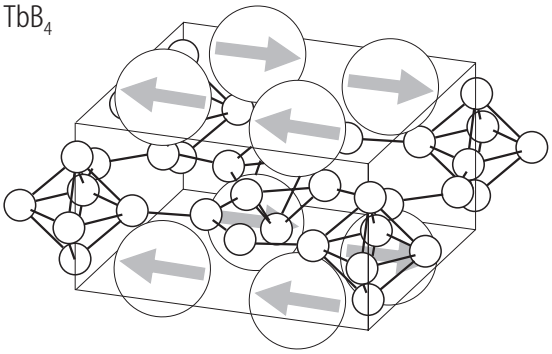

Fig. 6.

TbB_4. Single crystal. Temperature dependence of the reciprocal magnetic susceptibilities $\chi_{\parallel}^{-1}$ and $\chi_{\perp}^{-1}$ (H = 3000 Oe) [81G]. χ_g in CGS-emu.

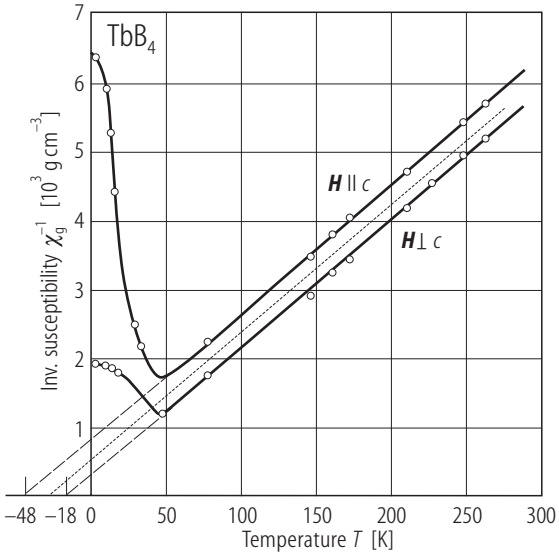

Fig. 7.

TbB_4. Single crystal. Variation of the specific magnetization as a function of field applied perpendicular to the *c* axis at 4.2 K [81G].

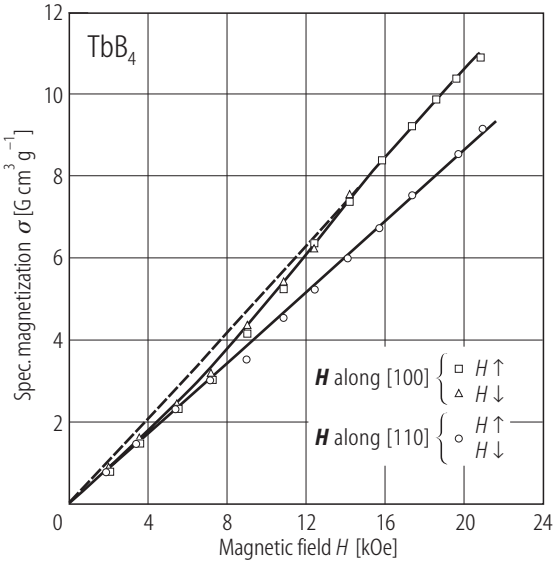

Fig. 8.

HoB_4. Temperature dependence of the reciprocal magnetic susceptibilities $\chi_{\|}^{-1}$ and $\chi_{\perp}^{-1}$(H = 3000 Oe) [81G].

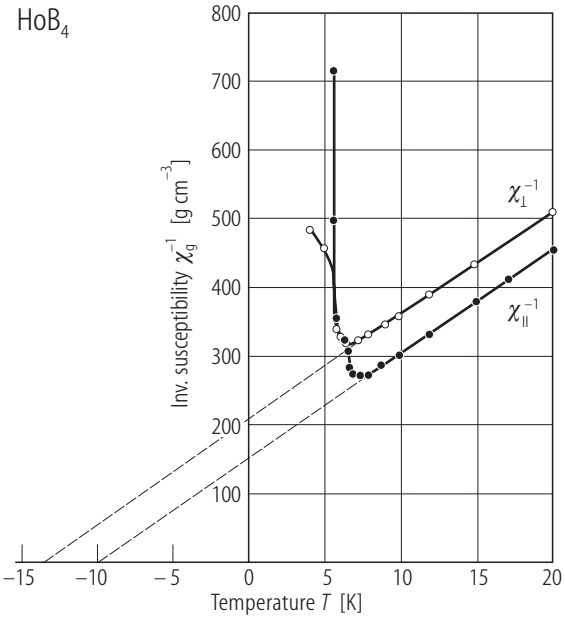

Fig. 9.

HoB_4. Variation of the magnetic moment per Ho ion as a function of field applied parallel to the *c* axis at 2.25 K and 4.2 K [81G].

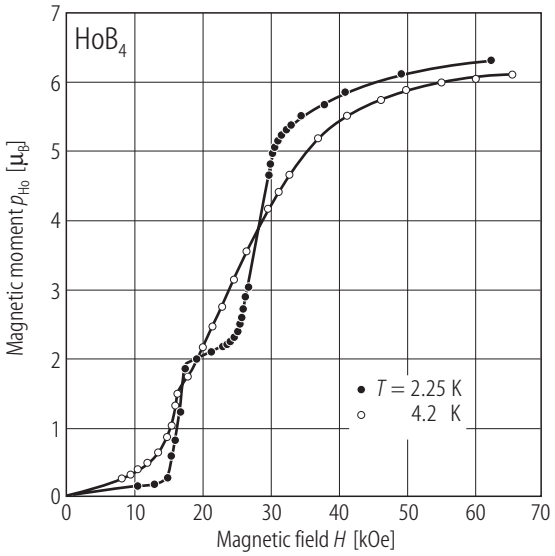

Fig. 10.

HoB_4. Variation of the magnetic moment per Ho ion as a function of field applied normal to the *c* axis at different temperatures [81G].

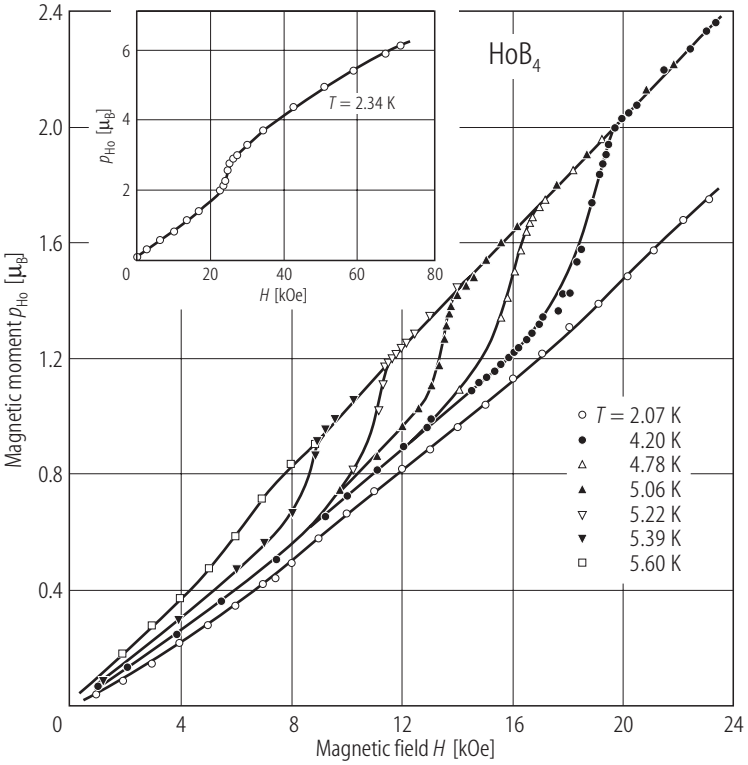

Fig. 11.

ErB_4. Antiferromagnetic structure with the magnetic moments oriented parallel to the *c* axis [81W].

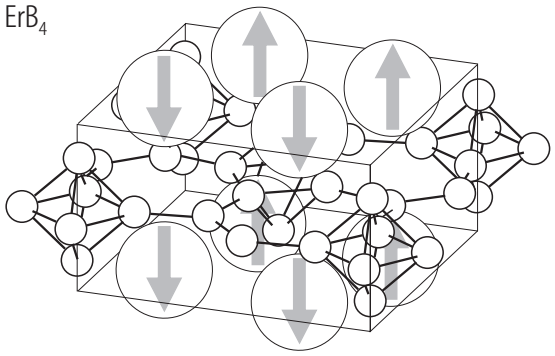

Fig. 12.

ErB_4. Magnetic phase diagram in the field-temperature space.